Optimal Point Shifting based on Virtual Impedance for Flexible Power Point Tracking and Power Reservation of PV Systems

Yeqin Wang[1], Xiuxia Liu[1], and Cui Wang[1]

[1]Affiliation not available

September 10, 2024

Abstract

In this letter, to handle the over-generation issue of photovoltaic (PV) systems based on maximal power point tracking (MPPT) algorithms, and to provide the power reservation for power grids, an optimal point shifting design based on virtual impedance is proposed for PV systems with flexible power point tracking. With the introduction of the virtual impedance, the virtual PV power is provided to auto-shift optimal power points on PV power-voltage curves. With a MPPT algorithm applied to the virtual PV power, the actual PV power is auto-turned without the estimation of maximum available PV power. The proposed design is validated through simulation studies of a PV-battery charging system and experimental studies of a grid-tied PV system, where both the overcharging of the battery and the over PV power generation are effectively avoided by reducing actual PV power according to the increasing of the battery SOC or the grid RMS voltage, respectively.

Optimal Point Shifting based on Virtual Impedance for Flexible Power Point Tracking and Power Reservation of PV Systems

Yeqin Wang, *Member, IEEE,* Xiuxia Liu, Cui Wang

***Abstract*—In this letter, to handle the over-generation issue of photovoltaic (PV) systems based on maximal power point tracking (MPPT) algorithms, and to provide the power reservation for power grids, an optimal point shifting design based on virtual impedance is proposed for PV systems with flexible power point tracking. With the introduction of the virtual impedance, the virtual PV power is provided to auto-shift optimal power points on PV power-voltage curves. With a MPPT algorithm applied to the virtual PV power, the actual PV power is auto-turned without the estimation of maximum available PV power. The proposed design is validated through simulation studies of a PV-battery charging system and experimental studies of a grid-tied PV system, where both the over-charging of the battery and the over PV power generation are effectively avoided by reducing actual PV power according to the increasing of the battery SOC or the grid RMS voltage, respectively.**

***Index Terms*—Optimal point shifting, virtual impedance, virtual PV power, flexible power point tracking**

I. Introduction

Photovoltaic (PV) industry grows fast in recent years with the significant fallen of both manufacture costs and installation costs. One of major PV applications is connected to distributed grids. PV sources are also used for the charging of energy storage devices. Currently, non-model based maximal power point tracking (MPPT) algorithms, such as, perturb and observe (P&O) algorithms, gradient-based extremum seeking (ES) algorithms, incremental conductance algorithms, are most common for PV systems with the maximum power acquisition.

With high penetration level of PV sources, distributed grids may face overloading issue or over voltage issue due to the continuous MPPT mode operation of PV systems. PV power curtailment is investigated to handle this issue [1]. For example, a reliable curtailment solution is provided by a modified over-voltage protection scheme to accommodate additional PV capacity [2]. A droop-based active power curtailment is proposed in [3] to droop the maximum available PV power. However, it is not easy to estimate maximum available PV power for PV power curtailment methods with the fast varying of solar irradiance [1]. The droop-based active power curtailment [3] is not compatible to non-model based MPPT algorithms.

Yeqin Wang is with the School of Automotive Studies, Tongji University, Shanghai, 201804, China.

Xiuxia Liu is with the Sichuan Institute for Advanced Study on Culture and Education, Sichuan Normal University, Chendu, 610066, China

Cui Wang is with the School of Electrical Engineering, Nanchang Institute of Technology, Nanchang 330099, China.

Corresponding author:Yeqin Wang (e-mail: yeqin.wang.1987@ieee.org)

Recently, researchers focus on "flexible power point tracking (FPPT)" algorithms, or "constant power generation (CPG)" algorithms to deal with the over-generation issue for PV systems. Three CPG control solutions are benchmarked in [4], where the CPG algorithm based on the P&O algorithm has high robustness for the operation at left side of the power-voltage curves. A "sample and hold" MPPT for maximum power estimation and the CPG algorithm for the constant power reservation is proposed in [5], where a large DC-bus buffer is required for frequently mode switching. A multi-mode FPPT algorithm is proposed in [6] to achieve MPPT and non-MPPT operations for PV systems, where a proportional-integral (PI) controller is designed to calculate the PV voltage deviation for power reducing. With the capability of flexible power output for PV systems, FPPT algorithms also can provide the power reservation for power grids, as discussed in [7]. Currently, FPPT or CPG algorithms are only based on the modification of the conventional P&O algorithm, and mode switching is usually required.

In this letter, an optimal point shifting design based on virtual impedance is proposed for PV systems with FPPT. With the similar design philosophy of FPPT, the concept of FPPT is also adopted in this letter. The virtual impedance is designed based on the basic impedance and the impedance factor, where the impedance factor can be designed based on the application requirements, e.g., battery voltage or battery SOC for battery charging scenarios, grid frequency/voltage for microgrid operation or grid-tied operation, or a higher level controller. The main contributions of this letter are summarized as follows.

- The virtual PV powers are provided and optimized by a MPPT algorithm to auto-shift optimal operation points of PV sources, where the virtual PV powers are calculated by the introduction of the virtual impedance.
- Compared to previous FPPT algorithms, the proposed FPPT design is targeted to the PV source, not MPPT algorithms. The proposed design is compatible with various MPPT algorithms under different solar irradiance levels without the estimation of maximum available PV power.
- A unified control scheme is achieved without mode switching for auto-shifting operation points of PV source. Also, with the introduction of power reservation factor in the virtual impedance factor, the power reservation of PV systems can be achieved through the proposed design.

The rest of this letter is organized as follows. The detailed optimal point shifting design based on virtual impedance is

proposed in Section II. The effectiveness of the proposed approach is validated through both the simulation studies in Section III and the experimental studies in Section IV, with concluding remarks made in Section V.

II. Optimal Point Shifting Design Based on Virtual Impedance

The original $P_{pv}-V_{pv}$ curves of a PV source under different solar irradiance levels are shown in Fig. 1. Most of MPPT algorithms continuously track optimal power points without the model of the PV source. In this section, a virtual impedance design is proposed to shift optimal power points for the scenarios with power decreasing requirement. Different PV applications are considered.

A. Virtual PV Power Calculation based on Virtual Impedance

The virtual impedance is designed as

$$V_{pvm} = V_{pv} - I_{pv}R_v \tag{1}$$

where V_{pv} and I_{pv} are actual output voltage and output current of the PV source respectively, which are usually measurable, V_{pvm} is the modified PV output voltage, and R_v is the virtual impedance can be design with

$$R_v = \alpha R_0 \tag{2}$$

where $R_0 = \frac{V_{oc}}{I_{sc}}$ is a basic impedance, and V_{oc} and I_{sc} are corresponding open-circuit voltage and short-circuit current of the PV source at the standard test condition respectively. α is an impedance factor and needs to be designed based on the application requirements, e.g., battery voltage or battery SOC for battery charging scenarios, or grid frequency/voltage for microgrid operation or grid-tied operation to facilitate optimal point or non-optimal point operation.

The virtual PV power P_{pvm} can be calculated as

$$P_{pvm} = V_{pvm}I_{pv}. \tag{3}$$

In this design, α can be $\alpha \geq 0$ or $\alpha \leq 0$, it depends on the left or right direction shifting of the optimal points. In this letter, $\alpha \geq 0$ with right-shifting is considered. When $\alpha = 0$, the normal MPPT is adopted, if α increases, the virtual maximal power point will be achieved. The normalization output curves for a PV source under a certain level of solar irradiance with different α is shown in Fig. 2. It creates several "virtual" optimal points, e.g., $O_1 \sim O_3$. If the $\alpha = 3$ is selected, the "virtual" optimal point can cause 80 % power droop on the actual optimal point O_o. By tracking these "virtual" optimal points through MPPT algorithms, the actual PV output power can be auto-tuned. Noted that optimal point shifting design based on virtual impedance can be applied to different solar irradiance levels shown in Fig. 1 without the estimation of maximum available PV power.

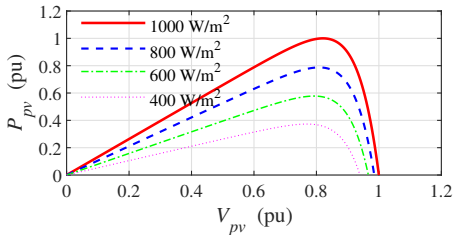

Fig. 1. The original $P_{pv} - V_{pv}$ curves with different solar irradiance levels

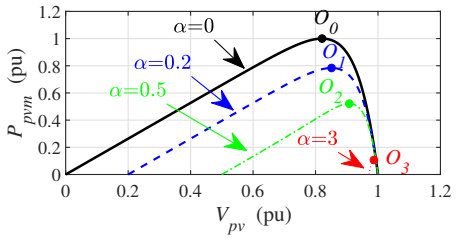

Fig. 2. The $P_{pvm} - V_{pv}$ curves with the proposed virtual impedance design under a certain level of solar irradiance

B. Design of Virtual Impedance Factor for PV System Applications

Here is a design example for the virtual impedance factor α as

$$\alpha = k\text{Sat}\left(\frac{X - X_0}{X_{max} - X_0}\right) + k_0 \tag{4}$$

where "X" represents a system parameter used to design the virtual impedance factor α. X_0 is the trigger point when PV power should be reduced, X_{max} is the maximum design target of X, and k is a design gain to decide how fast the power decreases from the optimal point, and k_0 is a power reservation factor used for the power reservation. The saturation function

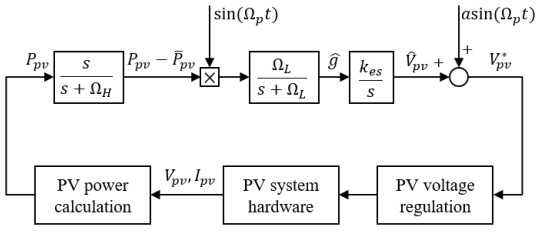

(a) Original ES optimization

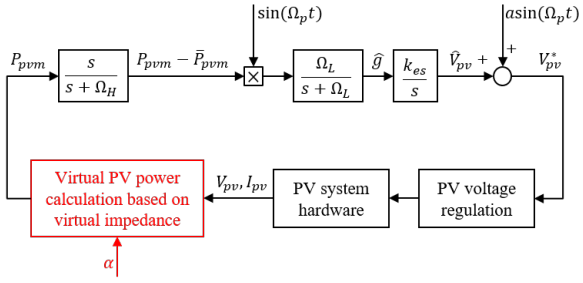

(b) Virtual impedance design-based ES optimization

Fig. 3. An application design based on the proposed design

TABLE I
SYSTEM PARAMETERS AND CONTROL PARAMETERS FOR SIMULATION STUDIES

System Para.	Values	Control Para.	Values
PV rated power	5 kW	R_0	13 Ω
PV rated voltage	250 V	SOC_0	0.9
Nominal Battery voltage	320 V	SOC_{max}	0.95
Battery capacity	8 Ah	k	4

Sat(•) is defined as

$$\text{Sat}(x) = \begin{cases} x, & x \geq 0, \\ 0, & x < 0. \end{cases} \tag{5}$$

If battery charging scenarios are considered, X can be selected as the battery state of charge (SOC) or the battery voltage V_{bat} to prevent the over-charging of batteries. If a grid-tied PV inverter under microgrid operation or grid-tied operation is considered, X can be selected as the grid frequency ω or the grid RMS voltage V_{ac} to prevent the over-generation of PV sources.

For example, for a grid-tied PV inverter in low-voltage power networks, α can be designed as

$$\alpha = k\text{Sat}\left(\frac{V_{ac} - V_{ac0}}{V_{acmax} - V_{ac}}\right) + k_0. \tag{6}$$

Considering $k_0 = 0$, if $V_{ac} \leq V_{ac0}$, the normal MPPT mode is achieved with $\alpha = 0$; if $V_{ac} > V_{ac0}$, with the increasing of V_{ac}, α increases accordingly, and the optimal point of the virtual PV power shifts to right to reduce the PV output power. k_0 can be designed to provide additional power reservation or ancillary service. If $k_0 > 0$, some PV power can be reserved, and if power networks need more power, k_0 can be set to a smaller value or 0 to release the reserved power. Noted that the virtual impedance factor α can be designed based on the other system parameters, or by a higher level controller.

C. Application Design

An application design is shown in Fig. 3, where the gradient-based ES algorithm is considered for maximum power acquisition. The detailed implementation of the gradient-based ES algorithm can be found in [8]. Compared to the original ES optimization in Fig. 3(a), a virtual PV power calculation block based on virtual impedance shown in Fig. 3(b) is considered to instead the original PV power calculation block. With the increasing of α, optimal points of the virtual PV power shifts to right. Though, the ES algorithm always tracks optimal power points of virtual PV power-voltage curves, the actual PV power can be reduced with the proposed design.

III. SIMULATION STUDIES OF PV-BATTERY CHARGING SYSTEM

In this studies, a PV-battery charging system is considered for simulation studies, where a PV source is used to charge a battery through a dc-dc converter. The battery SOC is used to design α to demonstrate the proposed design. The system parameters and control parameters are shown in Table I.

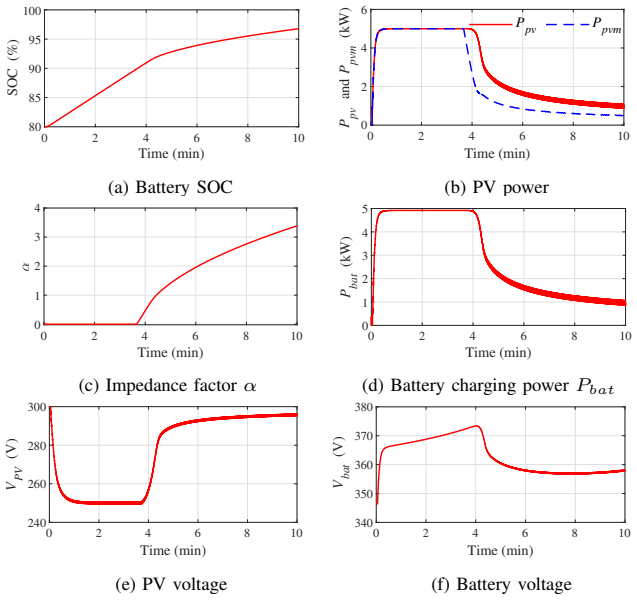

Fig. 4. Simulation results of battery charging.

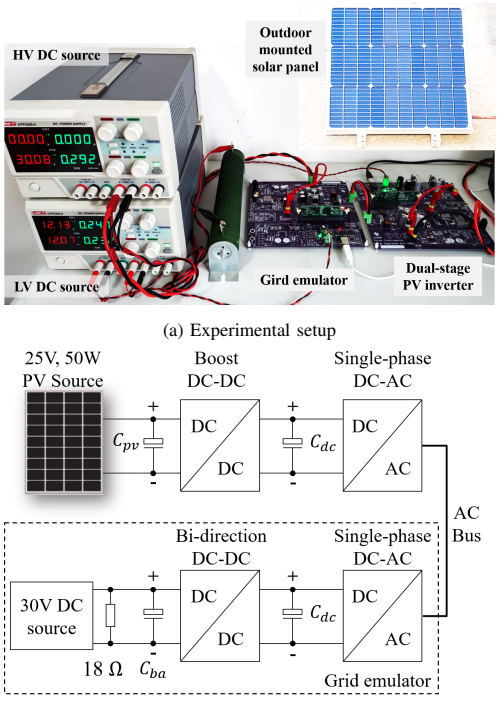

Fig. 5. Experimental setup of a dual-stage PV inverter connected to a grid emulator.

TABLE II
SYSTEM PARAMETERS AND CONTROL PARAMETERS FOR EXPERIMENTAL STUDIES

System Para.	Values	Control Para.	Values
PV rated power	50 W	R_0	13 Ω
PV rated voltage	25 V	V_{ac0}	23 V_{rms}
Rated grid voltage	22 V_{rms}	V_{acmax}	25 V_{rms}
Rated grid frequency	50 Hz	k	4
DC voltage	40 V	k_{es}	$\frac{1}{1+0.75\alpha}$

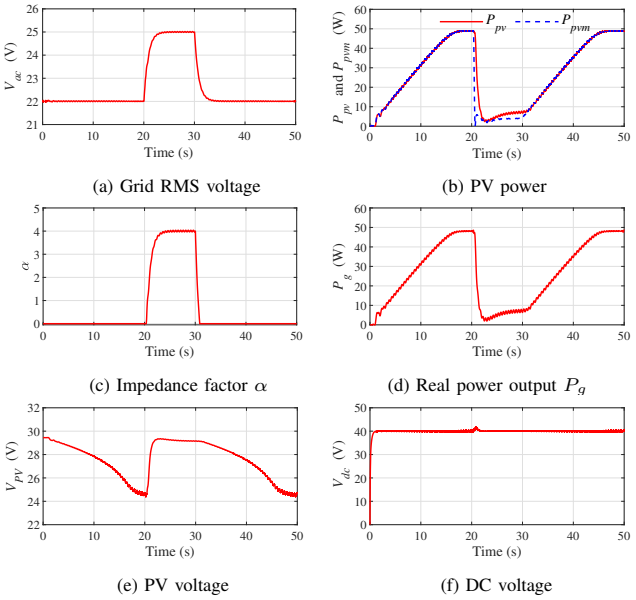

Fig. 6. Case I: Experimental results with high solar irradiance.

The simulation results are shown in Fig. 4. Initially, the battery SOC is with 0.8, and lower than SOC_0, and the charging system operates at MPPT mode with $\alpha = 0$, as shown in Figs. 4(a) and 4(c). The PV power reaches maximum value quickly, and the virtual PV power equals to the actual PV power, as shown in Figs. 4(b). The battery charging power is slightly lower than the actual PV power shown in Fig. 4(d). When the battery SOC reaches to SOC_0 at $t = 3.7$ min, the battery charging power should be reduced to avoid over-charging. With the increasing of the battery SOC, the impedance factor α increases gradually. Both the PV power and the battery charging power decrease gradually. When battery SOC reaches to 0.97 at $t = 10$ min, α is around 3.4, and the battery charging power is around 0.9 kW, already decreases 82%. The PV voltage follows the pattern of the actual PV power, and the battery voltage follows the pattern of the battery charging power, as shown in Figs. 4(e) and 4(f), respectively. Therefore, the FPPT operation of a PV source is achieved through the proposed design for the PV-battery charging system.

IV. Experimental Studies of Grid-tied PV System

To further validate the proposed FPPT, a experimental testbed consisting of a grid-tied dual-stage PV inverter connected to a grid emulator is developed, as shown in Fig. 5, where the grid-tied PV system consists of a 50 W solar panel, a boost dc-dc converter and a single-phase dc-ac converter. The grid RMS voltage is used to design α to validate the proposed design. The system parameters and control parameters are shown in Table II.

A. Case I: With High Solar Irradiance

In this Case, an increase of grid RMS voltage is considered between 20~30 s. The experimental results are shown in Fig. 6. Initially, the grid RMS voltage is with 22 V_{rms} shown in Fig. 6(a), and the maximum power acquisition of PV power is achieved from 1 s to 17 s, as shown Fig. 6(b). Where the virtual PV power equals to the actual PV power initially. The real power output P_g is slightly lower than the actual PV power shown in Fig. 6(d). At 20~30 s, with the increase of the grid RMS voltage, the impedance factor α increases to 4 accordingly, as shown in Fig. 6(c). Both the actual PV power and the virtual PV power decrease quickly. When $\alpha = 4$, the actual PV power is around 8 W, and decreases around 84 %. At $t = 30$ s, the grid RMS voltage decreases back to 22 V_{rms}, the grid-tied PV inverter is back to MPPT mode again with α decreasing to 0. During the whole experimental process, the PV voltage follows the pattern of the actual PV power, as shown in Fig. 6(e), and the DC bus voltage is always regulated to 40 V, as shown in Fig. 6(f). Therefore, the FPPT operation of a PV source is achieved through the proposed design for the grid-tied PV inverter.

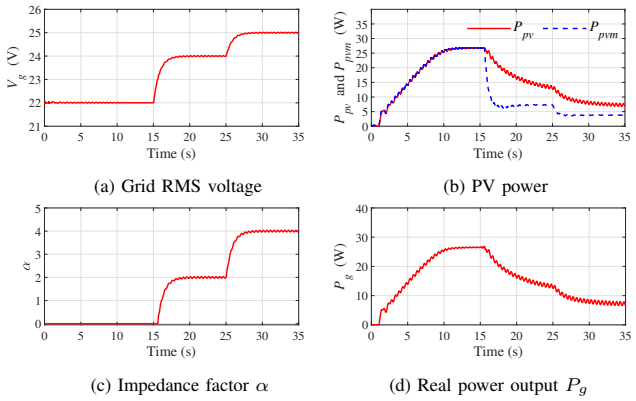

Fig. 7. Case II: Experimental results with low solar irradiance.

B. Case II: With Low Solar Irradiance

In this Case, with the same control parameters of the Case I, an increase of grid RMS voltage from 22 V_{rms} to 24 V_{rms}, then to 25 V_{rms}, with low solar irradiance is considered. The experimental results are shown in Fig. 7. With low solar irradiance, the maximum PV power only reaches to around 26 W, as shown in Fig. 7(b). When the RMS voltage reaches to 23 V_{rms} at $t = 15.6$ s, the impedance factor α starts to increase shown in Fig. 7(c), and both the actual PV power and the virtual PV power start to decrease, as shown in Fig. 7(b). When the RMS voltage reaches to 24 V_{rms}, the impedance factor α increases to 2, and the actual PV power decreases around 50 %. At 25~35 s, with the increasing of the grid RMS voltage again, the impedance factor α increases to 4 accordingly, and the actual PV power is around 7 W, and decreases around 73 %.

Because the proposed design based on virtual impedance has nonlinear effects of the power decreasing, and the power decreasing rate varies at different levels of solar irradiance. Under higher solar irradiance, the power decreasing rate is higher, and under lower solar irradiance, it is lower.

V. Conclusion

In this letter, an optimal point shifting design based on virtual impedance and virtual PV power has been proposed with FPPT to handle the over-generation issue or provide power reservation for PV systems. The virtual impedance is designed based on the basic impedance and the impedance factor, where the impedance factor can be designed based on the application requirements, and the virtual PV power is calculated by the introduction of the virtual impedance. With the ES-based MPPT algorithm applied to the virtual PV power, PV power operation points are shifted without the estimation of maximum available PV power. The effectiveness of the proposed design has been validated through both simulation and experimental studies.

References

[1] J. Hu, Z. Li, J. Zhu, and J. M. Guerrero, "Voltage stabilization: A critical step toward high photovoltaic penetration," *IEEE Ind. Electron. Mag.*, vol. 13, no. 2, pp. 17–30, Jun. 2019.

[2] O. Gagrica, P. H. Nguyen, W. L. Kling, and T. Uhl, "Microinverter curtailment strategy for increasing photovoltaic penetration in low-voltage networks," *IEEE Trans. Sustain. Energy*, vol. 6, no. 2, pp. 369–379, Apr. 2015.

[3] R. Tonkoski, L. Lopes, and T. El-Fouly, "Coordinated active power curtailment of grid connected PV inverters for overvoltage prevention," *IEEE Trans. Sustain. Energy*, vol. 2, no. 2, pp. 139–147, Apr. 2011.

[4] A. Sangwongwanich, Y. Yang, F. Blaabjerg, and H. Wang, "Benchmarking of constant power generation strategies for single-phase grid-connected photovoltaic systems," *IEEE Trans. Ind. Appl.*, vol. 54, no. 1, pp. 447–457, Jan./Feb. 2018.

[5] A. Sangwongwanich, Y. Yang, and F. Blaabjerg, "A sensorless power reserve control strategy for two-stage grid-connected PV systems," *IEEE Trans. Power Electron.*, vol. 32, no. 11, pp. 8559–8569, Nov. 2017.

[6] H. D. Tafti, C. D. Townsend, G. Konstantinou, and J. Pou, "A multi-mode flexible power point tracking algorithm for photovoltaic power plants," *IEEE Trans. Power Electron.*, vol. 34, no. 6, pp. 5038–5042, Jun. 2019.

[7] M. Haghighat, M. Niroomand, H. D. Tafti, C. D. Townsend, and T. Fernando, "A review of state-of-the-art flexible power point tracking algorithms in photovoltaic systems for grid support: Classification and application," *Journal of Modern Power Systems and Clean Energy*, vol. 12, no. 1, pp. 1–21, Jan. 2024.

[8] Y. Wang and B. Ren, "Fault ride-through enhancement for grid-tied PV systems with robust control," *IEEE Trans. Ind. Electron.*, vol. 65, no. 3, pp. 2302–2312, Mar. 2018.